FRONTIERS OF PHYSICS

VIEW & PERSPECTIVE
Volume 18 / Issue 5 / 53601 / 2023

Moisture influence in emerging neuromorphic device

Wenhua Wang, Guangdong Zhou†

College of Artificial Intelligence, Southwest University, Chongqing 400715, China
Corresponding author. E-mail: †zhougd@swu.edu.cn
Received December 9, 2022; accepted February 7, 2023

ABSTRACT

Conduction filament formation, redox reaction, and mobile ion migration in solid electrolytes underpin the memristive devices, all of which are partially influenced or fully dominated by the moisture. The moisture-based physical-chemistry mechanism provides an electric tunable method to create enough dissociate conductance states for neuromorphic computing, but overconcentration moisture will corrode electrode and then causes device invalidation. This perspective goal is that surveys the moisture-dependency of dynamic at interfaces or/and switching function layer, clarifies the bottlenecks that the memristive device facing in terms of water molecule-related reaction, and gives the possible solutions.

Keywords memristor, moisture, redox reaction, oxide, interface engineering

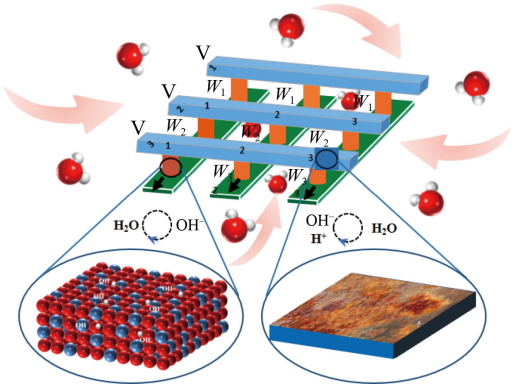

Contents

1 Introduction

Memristor is one of emerging electronic device for neuromorphic computing system [1]. The memristor characterized by a resistance switching (RS) displays ultralong information storage (>10 years) [2], fast switching speed (<1 ns) [3], high on/off resistance ratio ($>10^6$), and high self-selectivity ($>10^{10}$) [4, 5]. Memristive devices can be classified to be (i) unipolar and bipolar [6, 7]; (ii) digital and analog [8, 9]; (iii) electrical transition mode [10]; and (iv) cation and anion-dominated one [11, 12]. Among them, ion-type memristors have been extensively investigated because the mobile ion under external stimulations can provide multi-dynamic process to build the variety of RS memory behaviors [13]. For instance, the RS memory behavior dominated by the migration and reaction of cations was called electrochemical metallization memories (ECMs) or conductive-bridge memristors (CBMs), while the RS memory behavior dominated by anion/oxygen ion reaction was defined to be valence change memories (VCMs) [14, 15]. Considering the storage information volatility and nonvolatility [16, 17], the electrochemical transition mode included two categories: one is nonvolatile memristor that could be used to implement synaptic functions and performed matrix multiplication and addition calculations [18–20], the other is volatile memristor featured by a spontaneous decay, enabling the type memristor to faithfully mimic short-term

*Special Topic: Materials, Mechanisms and Applications of Memristors (Eds.: Xiaobing Yan, Bin Gao & Qi Liu).

Higher Education Press

https://doi.org/10.1007/s11467-023-1272-8

synaptic plasticity (STP) or paired pulse facilitation (PPF) [21, 22].

Memristor have made milestone progress and breakthrough on both the physical mechanism and application [23–26]. Application of memristors The use of memristors in analogue circuits has been made possible by the emergence of new types of memristor-based hybrid circuits, enabling more circuit functions such as unconventional waveform generators and chaotic oscillators. In addition, memristors can be applied to artificial neural networks as artificial synaptic devices. Not only the formation and breakage of conducting filaments, the rate of redox reactions, ion mobility in solid electrolytes, nanosize and quantum effects [27, 28], but also environmental factors such as temperature, pressure and moisture are very critical for RS memory behavior construction [29–31]. All the RS behaviors can be ascribed to the coupling effect between ion and electron [12]. Oriented by this conception, Sun *et al.* [32] predicted that coupling between RS memory and capacitive state inevitably occurred in the memristor. Importantly, the submerging redox behavior induced a capacitive state was discovered when accurately controlling the concentration of protons, thus, the RS evolution map as the basis of water-based redox process was proposed to comprehend the memristive computing system [33].

In this perspective, we systematically survey the influence of moisture or relative humidity on ion/electron reaction dynamic in memristive devices, re-illuminate the corresponding internal physic mechanism, and give the possible solutions for the memristive device application neuromorphic computing system in future.

2 Protons in the switching function layer

The saturation current of the $\mathrm{Pt}|\mathrm{SrTiO_3}-\delta|\mathrm{Pt}$ memristor was increased by four orders when exposing to high relative moisture (RH) levels at room temperature [34]. The concentration and migration speed of protons are the major reason for the diversity of RS performance. For instance, Zhou *et al.* [35] reported that a coexistence of negative differential resistance (NDR) and RS memory effect when exposing the $\mathrm{Ag}|\mathrm{TiO}_x|\mathrm{FTO}$ memristor into different moisture levels. In fact, the oxygen ion (O^{2-}), adsorption oxygen (O_{ads}), and oxygen vacancy (V_o) were inevitably generated during oxide film preparation [12]. The O^{2-}, O_{ads}, and V_o could provide rich chemical sites to react with the water molecule in air [35], as shown in schematic diagram of Fig. 1(a). It notes that most oxides displayed an insulator property at the macroscale, but they possibly become ion/electron conductor at nanoscale [29]. This nanoscale-induced conduction effect was described as a hybrid ion-electron conductor. Many amorphous films have to nanopores structure. This unique structure enables the water molecules to easily

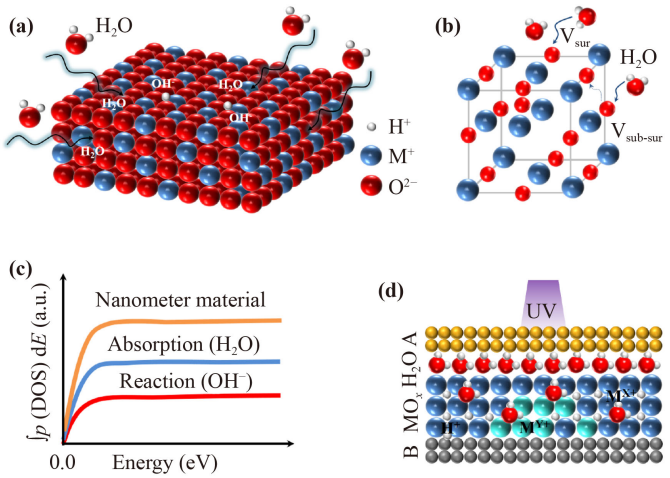

Fig. 1 **(a)** Schematic diagram of the reaction of water molecules with oxygen vacancies at the surface and interface [35]. Copyright © 2018, Wiley. **(b)** Schematic diagram of the distribution of surface oxygen vacancies (V_o^{sur}) and subsurface oxygen vacancies (V_o^{sub}) in oxides [39]. Copyright © 2014, American Physical Society. **(c)** The reaction of water molecules with nanostructures leading to a decrease in electron concentration [33]. Copyright © 2020, Nano Energy. **(d)** Switching of water molecules to modulate the valence state change of M under UV light. M^{x+}, M^{y+} and H^+ are represented by blue, cyan and white balls, top and bottom electrodes are represented by yellow and gray balls, respectively. a.u., arbitrary units [41]. Copyright © 2019, Springer Nature.

absorb in membrane and accelerates the corresponding chemical reaction [36]. For dense amorphous and crystalline materials, the adsorption water molecules make most of defective chemical reactions become possible. Surface gas-phase water molecules interact with oxygen and V_o in the lattice to generate $OH^{\cdot}$ and then migrate into the switching function film. The corresponding chemical reaction was given as follows [37]:

$$\mathrm{H_2O} + \mathrm{O_o^{\times}} + \mathrm{V_o^{\cdot\cdot}} \rightleftharpoons 2\mathrm{OH_o^{\cdot}}, \tag{1}$$

where $V_o^{\cdot\cdot}$ and $O_o^{\times}$ represent oxygen vacancies and oxygen in the lattice, respectively, and $OH_o^{\cdot}$ denotes the hydroxide free radicals. According to the chemical reaction of Eq. (1), water molecules are prone to hydrolysis reactions with $V_o^{\cdot\cdot}$ or oxygen at the interface under high $V_o^{\cdot\cdot}$ concentrations, and the water molecules permeation breaks the V_o conduction path and then alters the conductance [35, 38]. Li and Gao [39] stressed that the influence of the water molecule on the RS memory behavior was non-negligible. They have found that surface $V_o(V_o^{sur})$ and subsurface $V_o(V_o^{sub})$ provided the key chemical reaction site for the water molecule [Fig. 1(b)]. Water molecules reacted with the in turn causes the V_o^{sub} instability and followingly migrate from the subsurface to the surface, and finally become V_o^{sur}. And the processes promote the dissociation of water molecules in

turn. Therefore, the V_o^{sub} can promote the dissociation of water molecules directly or indirectly with the help of V_o^{sur}. Our previous work demonstrates that a large surface area of the TiO_x nanobelt can provide enough V_o^{sub} and V_o^{sur} for chemical interaction/dissociation of water [33]. First-principles calculations illustrate that the electron density decreased after water molecule absorption on the TiO_x nanobelt [Fig. 1(c)]. Water molecules are first adsorbed on the surface of the nanobelt and undergo redox reactions with V_o^{sur}, the large number of hydroxide ions, electrons and gases are generated on the surface of the nanobelt because of the occurrence of redox reaction processes [Eqs. (1) and (2)], resulting in a gradual decrease in electron concentration and change in the energy band structure [33]:

$$2H_2O \rightleftharpoons O_2 + 4H^+ + 4e^-. \tag{2}$$

In turn, the generated electrons can transfer between oxide film surface and water molecule.Valov *et al.* [29] and Wang *et al.* [28] have stressed that migration and interactions between ions and electrons can occur between water molecules and V_o [28, 29]. According to half-cell theory, the redox reaction of water molecules to generate hydroxide ions can be described by Eq. (3) [40]:

$$2H_2O + 2e^- \rightleftharpoons 2OH^- + H_2. \tag{3}$$

Therefore, the OH^- forms at the counter electrode and then keeps the charge electroneutrality in cation-transporting thin films. Meanwhile, the protons are also generated at interfaces. Zhou *et al.* [41] reported that a reaction between the oxide and water molecules to generate protons H^+, and photogenerated electrons cause a shift in the valence state of the oxide, resulting in a resistance shift. According to Eqs. (2) and (3), water molecules generate H^+ and OH^- without UV illumination, causing a valence change of the oxide at interfaces, while the multivalent oxide film can produce electrons and holes after UV illumination [Fig. 1(d)], this process can be ascribed by following formula [41]:

$$MO_x + h\nu \rightarrow MO_x^* + e^- + h^+. \tag{4}$$

Photogenerated electrons are excited in conduction band of the oxide film. When water molecules are adsorbed on the surface, photogenerated holes and water molecules will generate protons H^+ [Eq. (5)] and the H^+ distribution is modulated by the UV light [41]:

$$4h^+ + 2H_2O \rightarrow 4H^+ + O_2. \tag{5}$$

The reaction-generated protons and photogenerated electrons can lead to a change in the valence state of the oxide ions [Eq. (6)], resulting in the memristor resistance switching:

$$MO_x + ye^- + yH^+ \rightleftharpoons H_yMO_x, \tag{6}$$

$$O_2 + 2H^+ + 2e \rightarrow H_2O_2. \tag{7}$$

According to the action diagram of Fig. 1(d) for the water molecule and the polymorphic oxide, it can be concluded that the resistance switching is reversible, and the polymorphic oxide returns to its original state when the H^+ of the oxide layer reacts with the generated O_2 [Eqs. (7) and (2)], resulting in the device going from low resistive state (LRS) to high resistive state (HRS). The H_2O_2 splits into H_2O and O_2 under the UV illumination. The produced H_2O can also be used in the hydrolysis dissociation process under UV light.

The redox reaction of the water molecules, the interaction with defects such as V_o in the film, and the interaction between ions and electrons that occurs with oxygen and hydrogen can influence on the conductivity [37]. Water molecules in switching not only changes the energy band structure and the valence state of the oxide but also increases the conductivity. Therefore, introducing an appropriate concentration of water molecules in the oxide switching layer or the interfaces can promote the electric or optic switching dynamic construction for neuromorphic computing system [41, 42].

3 Water-based redox reaction in the memristor

Literatures have pointed out that the water mainly provided the required counter charge/reaction for anodic oxidation to trigger unique physic effects such as the coexistence of RS memory and NDR behaviors [27, 35, 43].

3.1 Redox reactions in electrochemical metallization memories

Aono *et al.* [43, 44] emphasized that the influence of the environmental factor on the RS behavior could not be neglected because the chemical interaction/dissociation of water on inert electrodes could impact the formation of metallic conducting filaments by anodic oxidation of electrochemical metallization memories [43, 44]. Utilizing the solid electrolyte of SiO_2 as a switching function layer, the adsorption of water molecules provides an electrode/to-charge reaction to promote the oxidation reaction at anode side [43]. The reaction of water molecules is responsible for the conducting path formation, which in turn regulates the resistance switching of SiO_2-based memristors. The influence of redox reactions on RS memory behavior is summarized in the following stages. After applying a certain bias voltage, the active electrode (M) of the anode undergoes an oxidation reaction in the electric field to produce M^{x+} that is described as following:

$$M + xe^- \rightarrow M^{x+}. \tag{8}$$

To first stage, no metal cation channel was established, and the ReRAM device was in the capacitive

state [Fig. 2(a)(i)]. According to the half-cell reaction, the sustained oxidation reaction at the electrochemically active electrode requires a counter-electrode reaction at the inert electrode to keep the electrochemical reaction electrically neutral [43]:

$$O_2 + 2H_2O + 4e^- \rightleftharpoons 4OH^-. \tag{9}$$

The counter-electrode reaction at the inert electrode [Eq. (9)] promotes the electrochemical oxidation of the active electrode, so that an increasing amount of M is oxidized, M^{x+} gradually migrates to the inert electrode (cathode) under the action of the electric field, and generates M atoms that gradually accumulate on the counter electrode [Eq. (10)] [Fig. 2(a)(ii)] [41]:

$$M^{x+} - xe^- \rightarrow M. \tag{10}$$

As the oxidization on the electrode increases, more M^{x+} is generated, and more M accumulates on the counter electrode to form a conductive channel, as shown in [Fig. 2(a)(iii)]. At this point, the ReRAM device switches from high resistive state (HRS) to low resistive state (LRS), mainly relying on water molecules to promote the oxidation of the active electrode (M) and the migration of moisture-enhanced ions along the grain boundaries of the oxide functional layer. Note that the moisture pressure partially dominates the threshold voltage, a high moisture pressure will lead to a small threshold voltage. The OH^- generated from the reaction at the counter electrode not only presents the modulation of the oxidation reaction of the active electrode but also acts as the mobile ion to form a conductive pathway between the top and bottom electrodes [Fig. 2(a)(iv)]. It is worth noting that the existence of the OH^- based conduction path makes the device with a higher current under the same bias voltage.

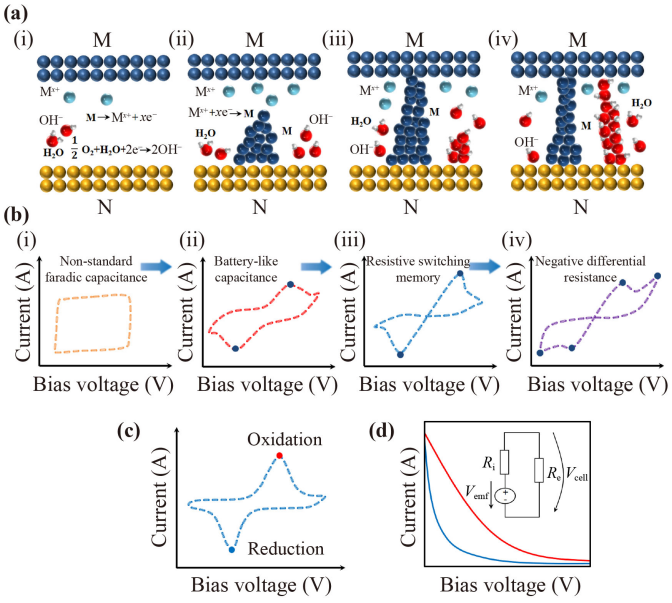

Fig. 2 **(a)** Schematic diagram of redox reactions in electrochemical metallization memories forming conductive paths. M^{x+} and M are represented by cyan and blue balls, top and bottom electrodes are represented by blue and yellow balls, respectively. a.u., arbitrary units [27, 43]. Copyright © 2021 and 2013, ACS Publications. **(b)** The evolution of the memristor from capacitive to memristor state [33]. Copyright © 2020, Nano Energy. **(c)** Water molecules induce oxidation and reduction peaks in the memristor. **(d)** The time evolution of the discharge current after SET and RESET operation is shown. Inset: simplified equivalent circuit model of a ReRAM device [46, 48]. Copyright © 2013, Springer Nature & Copyright © 2022, Cell Press.

3.2 Moisture and protons dynamics in the switching function layer

Most memristors are tested in air. Williams *et al.* [45] and Valov *et al.* [46] reported that redox reaction of water molecules severely affects the migration of oxygen vacancies and the formation of conducting filaments even at room temperature [45, 46]. Therefore, magnitude of relative humidity (RH) as efficiently tunable methods was used to construct various RS behavior and NDR coexistence at room temperature [Fig. 2(b)] [35]. After applying a positive bias voltage to the device, the capacitive state is observed in the memristor cell at RH = 0% [Fig. 2(b)(i)], the interaction between ions and electrons is faint and the memristor state cannot be observed, coupled with a weakening redox peak.

When the device is exposed to a humid environment and gradually increases the relative moisture, the device displays a battery-like capacitance (BLC) state that was governed by Eqs. (1) and (2). Thus, an obvious redox peak and an increased current emerges when the devices are tested in air [Fig. 2(b) (ii)]. An increase moisture concentration accelerates hydrolysis reaction and then triggers the resistance to switch, [Fig. 2(b)(iii)]. Interestingly, coexistence of NDR and RS behavior was obtained when the moisture increases to a certain range, [Fig. 2(b)(iv)]. This result illustrates that the coexistence of NDR and RS can be achieved at room temperature by the interaction between the ion and electron-based redox reaction.

The redox charge can be measured according to the redox peak [Fig. 2(c)]. The positions of the oxidation and reduction peaks are found according to the current–voltage curves (I–V). When the memristor reaches the oxidation peak and reduction peak current density (J_p), the memristor is set to short circuit according to the test circuit in Fig. 2(d) illustration. The number of charges (Q) can be obtained by integrating the area of the discharge current versus time, as shown in Fig. 2(d). The redox process is described by Eq. (11) [45–48]:

$$J_{p\text{-redox}} = 2.99 \cdot 10^5 \cdot Z^{\frac{3}{2}} C_{\text{redox}} \cdot \sqrt{\alpha \vartheta D_{\text{redox}}}, \tag{11}$$

where $J_{p\text{-redox}}$, Z, C_{redox}, α, ϑ and D_{redox} denote the redox

peak current value (A/cm^2), number of electrons transferred during the redox process, ion concentration (mol/cm^3), charge transfer coefficient, bias voltage scan rate, and ion diffusion coefficient (cm^2/s), respectively. The $J_{p\text{-redox}}$ can be obtained by integrating the area of the discharge current versus time. According to the Nernst–Einstein relation, the value of D_{redox} can always be calculated in Eq. (11) [46]:

$$\mu_{\text{redox}} = \frac{D_{\text{redox}} Ze}{K_B T}, \tag{12}$$

where the μ_{redox}, K_B, and T are the ion mobility [$cm^2/(V \cdot s)$], Boltzmann constant, and temperature, respectively. Q can be obtained by integrating the area of the discharge current versus time and D_{redox}. The values of C_{redox} and μ_{redox} can be calculated from Eqs. (11) and (12). Thus, the relationship between C_{redox} and D_{redox} and μ_{redox} can be obtained from the memristor evolution process [48].

4 Utilizing the water-based reaction to optimize the memristive application

The change concentration and migration speed have a significant impact on the application of a memristor [49]. The modulation of moisture on RS behavior can apply to various types of memristors and has profound effects from high-density storage and memory logic gates to neuromorphic chips [50]. Considering that some devices are more sensitive to moisture, strongly dependent on moisture pressure and that the dependence is reversible, moisture-sensitive memristors can be also used as high-precision moisture sensors and resistive switches for induced humidity control 43. Moreover, the moisture related RS behaviors could be employed to construct the ultralow energy computing, because the water-related reaction reduces the extra energy supply. The large resistance change was ascribed to the generation and migration of protons that mainly originated from water dissociation. As shown in Fig. 3, the memristor evolution stage from nonstandard faradic capacitance (NFC) to battery-like capacitance (BLC) and resistive switching state (RS) is discovered under different moisture contents. In the initial state (RH = 0%), proton generation and migration are restricted, and the interaction between ions and electrons is very weak, which induces the memristor in the NFC stage. In a moist environment, OH^- is generated due to the redox reaction of water, which is suspended on the V_o^{sur} of the oxide film, resulting in the device evolving from NFC to BLC [9]. With the increase in moisture level, intensifying the interaction between electrons and ion transfer and migration of OH^- ions triggers the RS behavior of the device. In addition, moisture was responsible for the coexistence of NDR and resistive switching in $Ag/TiO_x/FTO$ devices [35], implying that the RS behavior of the memristor can be driven by modulating moisture levels.

Moisture not only modulates the RS behavior but also affects chip preparation [51, 52]. As an important component of integrated circuits, the preparation process and packaging technology of chips have received much attention [53]. The adsorption and interaction of water molecules bring both opportunities and challenges in the fabrication of memristor chips [54]. In the chip preparation process, it is impossible to avoid the generation of defective states, protons (H^+ and OH^-) generated by the reaction of defects with water molecules. The concentration changes and motion of protons have a nonnegligible influence on the preparation of chips, as shown in Fig. 3. Importantly, the hydroxyl hanging bond on the Si wafer can improve the contact quality between the external memristor array with a Cu or Al pattern. Therefore, water-based reaction on the surface of the switching function layer can bring light future for memristors chip applications. Without adsorbed water molecules, the device is susceptible to breakdown at high scan voltages, and even if it is not, the device has no RS behavior, thus, water molecules in the chip packaging test are urgently needed [27]. However, due to the strong corrosive nature of water molecules, the adsorption of water molecules also brings a challenge for memristive chip architecture [53]. Active metal electrodes are easily affected by corrosion due to the negative Gibbs formation energy of the oxide [55–57]. Thus, it is impossible to avoid water dissociation to corrode the electrode material, which reduces the retention rate and decreases the lifetime of the device.

Protons generated by water adsorption, dissociation and migration are responsible for the RS behavior of memristors. It can be used to realize memory logic functions. Zhou *et al.* [58] designed storage logic gates and an information display of $Ag|MnO_x|Ag$ memristor modulation by moisture levels and electrical signals [58]. According to Fig. 3 schematic diagram, it can be concluded that logic gates are feasible. When the output current (I_{out}) exceeds I_1, the logic state is defined as 1, corresponding to the "OR" logic gate, the state is defined as zero. In addition, when I_{out} exceeds I_2, it corresponds to the "AND" logic gate. It should be emphasized that only the simultaneous application of the electrical signal and moisture level can make the "AND" logic gate (Fig. 3) [58]. In addition, the device stability is critical in the application of logic operations with memristors. Zhou et al. further verified the stability of the device under the dual operation of modulating moisture and electrical signal, and detected that the output value of this device indicating that the device holds stable conductance state under specific moisture levels. Thus, memory logical gates could be realized by control the moisture level.

Assisted by water dissociation on the surface of the

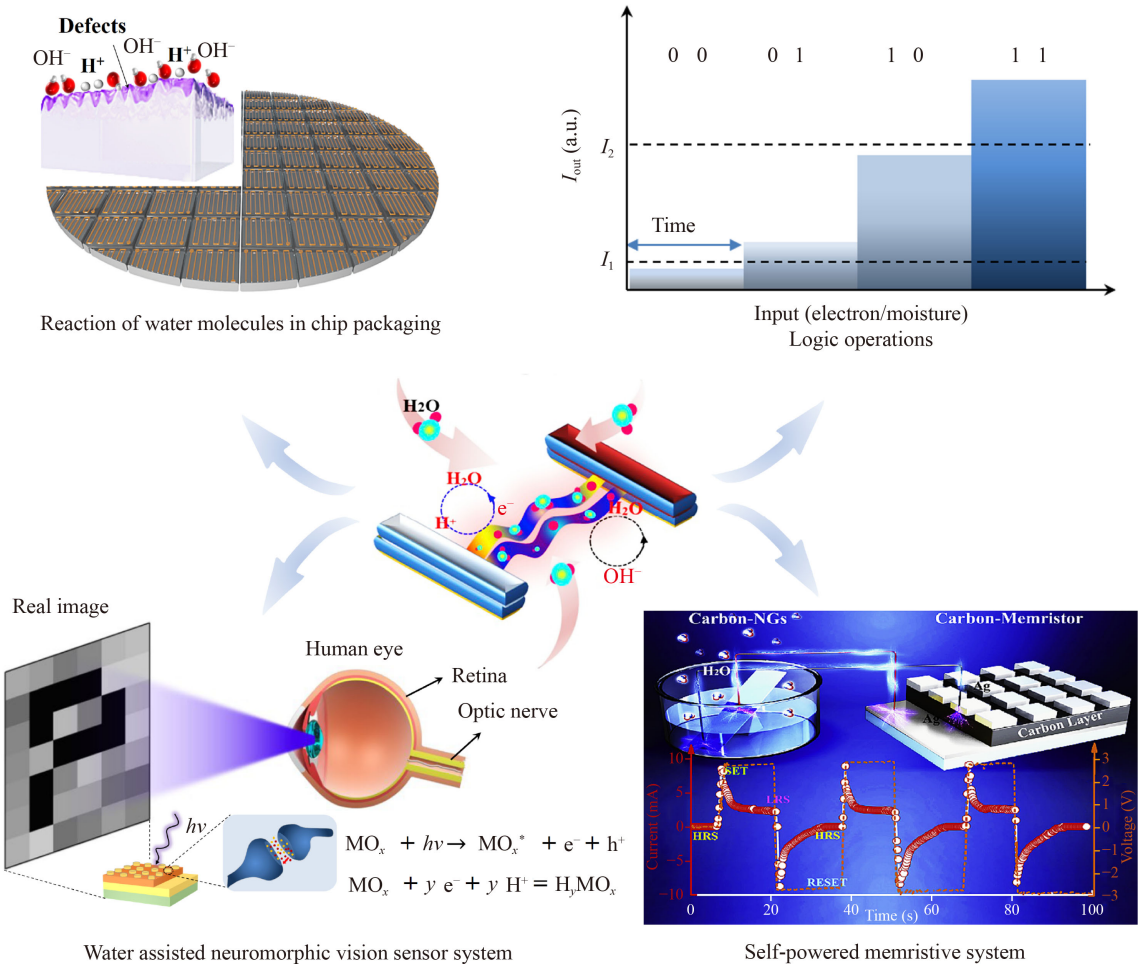

Fig. 3 Schematic diagram of the role of moisture for memristor applications [31, 39, 49, 55, 56]. Moisture induced memristor evolution stage. Copyright © 2020, Nano Energy; The water-based reaction in chip packaging. Copyright © 2021, ACS publications; Effect of moisture on memristor in logic operations. Copyright © 2019, the Royal Society of Chemistry; Water molecule assisted neuromorphic vision sensor system. Copyright © 2019, Springer Nature; Preparation of self-powered memristor using the influence of water molecules. Copyright © 2019, Nano Energy.

oxide functional layer, the valance change is sensitive to external UV stimulation. Utilizing this sensor to mimic the dynamics of synapses, a neuromorphic vision sensor that has a low delay time, high speed, and low consumption was developed. The corresponding dynamics are summarized as follows: multivalentroxide (MO_x) can produce electrons and holes in the oxide film under UV illumination, in which water molecules can generate protons (H^+) through redox reactions, and protons react with oxides and electrons under the action of UV light, finally changing the valence state of the oxide and triggering the RS behavior of the device. Meanwhile, the polymorphic oxide returns to its original state when the H^+ of the oxide layer reacts with the generated O_2 [41]. Thus, under UV light, the modulation of water molecules on the oxide memristor can be applied to the neuromorphic visual system. Image sensing, memory functions, and neuromorphic vision preprocessing are achieved by the interaction of water molecules with the device. Thus, water molecule-modulated photoelectric switch devices play a visual role in neuromorphic visual preprocessing and vision systems.

In addition, water dissociation on the oxide surface can accelerate the separation and distribution of positive/negative charge, thus, a stable output potential is generated during dissociation proceeds. Utilizing this stable output, the memristor as a passive device can be self-powered. The separation and distribution of positive/negative charges was realized using graphene-like carbon sheets. After integrating the graphene-like carbon-based nanogenerator into the Ag|Carbon|Ag memristor, the high resistance state (HRS), low resistance state (LRS), set and reset voltage were obtained [59].

5 Issues and suggested investigations

Water molecule is creating a fine optimization bright

future in memristor preparation, measurement, and performance. Moisture has important effects on the device logic operations, neuromorphic computing and chip packaging [60]. Because it not only modulate the electrochemical behavior, but also affect the switching performance.

Protons have become an inevitable part in oxide switching films. Complete removal the protons from the memristive devices becomes extremely difficult, but introducing a suitable concentration of protons is more favorable for triggering the RS occurrence. The generation of protons on the surface of the switching function layer can shorten the time of the forming process because the nanoscale conduction path and localization conduction region are first bridged by protons [33]. As previous summary, protons migrate along the grain boundary defects or even penetrate the switching function layer through the diffusing effect and scattering effect under external stimulations. Employing the coupling between ions and protons to obtain, unique physical behavior, such as negative differential resistance (NDR) [61], negative photoconductance (NPC) and self-rectifying RS memory effects, the memristor can meet the various requirements of applications [33].

The generation and incorporation of proton provides multidynamic RS memory processing. The environmental conditions during device preparation and testing have a non-negligible effect on the result. For the same device, different humidity levels lead to the discrepancies of measurement results. For instance, the Ta_2O_5- and SiO_2-based does not set from HRS to LRS even under large voltage bias in high vacuum, while the RS memory is easily obtained under moisture ambient [43, 44]. It notes that most electrical measurements of the memristive devices were exposed into into air ambient with a relative humidity level of 35%–65%. The levels of moisture profoundly influence the electrical characteristics, such as forming voltage, device current, resistance ratio, and power consumption.

Thus, memristive devices show the variety of the RS memory behaviors can be comprehended by the water-based reaction dynamics under different moisture levels in air ambient. In addition, the preparation technics including the chemical vapor deposition (CVD), atomic layer deposition (ALD), and magnetron sputtering do not absolutely avoid the incorporation of water molecules. Therefore, exploring how to control the moisture concentration in the memristive devices becomes meaningful and necessary for the RS memory behaviors for chip packaging, stability, and reliability, as shown in Fig. 4 [49]. It notes that water can be used as a corrosive agent, and it can corrode the material of the device and reduce its retention. Thus, water molecule is not negligible in the chip technology. During the preparation and packaging of devices, even in a high vacuum environment, the generation of defect states (protons) is impossible to avoid, so the reaction between moisture and defects always occurs. The redox reaction originating from water molecules causes corrosion of the device electrodes and reduces the lifetime of the device. For the packaged electronic device, moisture can penetrate from the edge of the electrode and can pass through the protective layer film. After a certain period of penetration, the functional layer will still corrode [28].

Based above analysis on water-based physic mechanism, the critical issues and possible solving methods are discussed as follows (Fig. 4): (i) Should we introduce the high or low concentration of water to the switching electrolyte matrix or not, surface/subsurface. (ii) How to control the redox reaction between moistures and oxide films. iii) What is the origin of the physical-chemistry dynamics for the water rection in oxide film and surfaces.

To the first issue, high or low binding water to oxide switching electrolyte is determined by the metal valences, surface/subsurface oxygen vacancies, and moisture levels. Generally, water overconcentration causes conductance fluctuation, corrosion electrodes, and even computing invalidation. While a suitable concentration is beneficial because the generation of ions and electrons facilitates the conduction filament formation and even zero-energy consumption to power the computing system. To the second issue, the control water molecule reaction is very critical for obtaining high RS performance and ensuring normal computing implementation of neuromorphic chips. The high vacuum level of $< 10^{-5}$ is recommended during the oxide switching function layer preparation and electrical measurements are controlled in the relative humidity range of 20%–50%. To obtain unique physic effect such as NDR behaviors or building an interface-dependency light sensitive devices, the relative high moisture levels, necessary surface processing, and suitable energy band structure design should be considered. In addition, the ultra-large arrays-based chip under different packaging modes should consider the moisture influence, the RS performances under low moisture level are suggested.

To the third issue, the origin of the physical-chemistry dynamics is still in controversy because of the lack of deep investigation and solid evidence. The deep root of the RS memory behaviors will dominate this type device application in future computing system. A unified theory involving the re-definition of mathematical expression, electron/ion of localization effect, and multi-variable physic model, is urgently developed to offer tunable methods to guide the memristor-based neuromorphic computing hardware fabrication.

6 Conclusion

Water-based reaction exists in the process of device

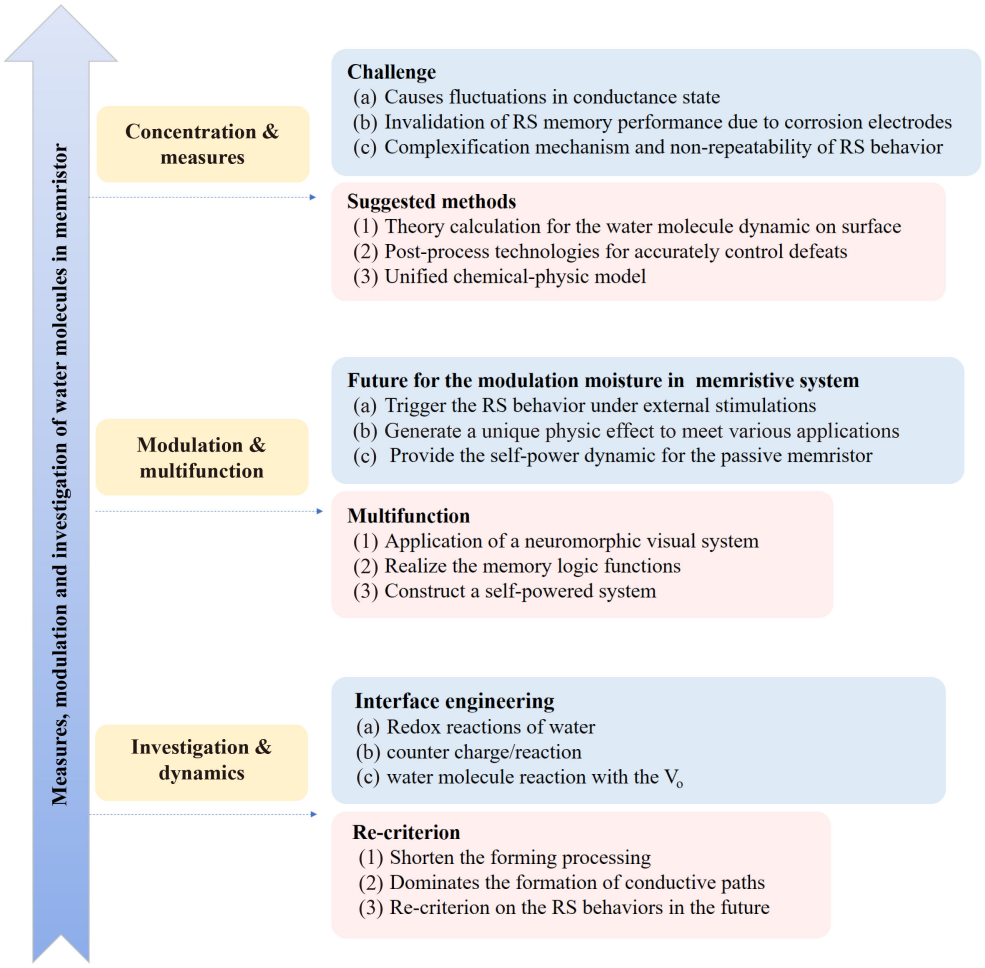

Fig. 4 Issues, suggested measures and investigation of water molecules in memristor.

preparation, testing, packaging, and application. The redox reaction of water molecules can not only trigger the electrochemical behavior of the device, but also modulate the conductivity value and RS behavior. The concentration, generation, and corresponding chemical physics dynamic model underpin the comprehension the water-related complex dynamics in memristive system. Challenges and bright future coexist for the proton effect in the RS function layer, and both utilization and control of the reaction dynamics, there are necessary for memristor-based applications to construct a unique physics effect for neuromorphic computing.

References

1. Z. R. Wang, C. Li, W. H. Song, M. Y. Rao, D. Belkin, Y. N. Li, P. Yan, H. Jiang, P. Lin, M. Hu, J. P. Strachan, N. Ge, M. Barnell, Q. Wu, A. G. Bartos, Q. R. Qiu, R. S. Williams, Q. F. Xia, and J. J. Yang, Reinforcement learning with analogue memristor arrays, *Nat. Electron.* 459(2036), 2 (3), 115 (2019)
2. Y. F. Pei, Z. Q. Li, B. Li, Y. Zhao, H. He, L. Yan, X. Y. Li, J. J. Wang, Z. Zhao, Y. Sun, Z. Y. Zhou, J. H. Zhao, R. Guo, J. S. Chen, and X. B. Yan, A multifunctional and efficient artificial visual perception nervous system with Sb_2Se_3/CdS-Core/Shell (SC) nanorod arrays optoelectronic memristor, *Adv. Funct. Mater.* 32(29), 2203454 (2022)
3. Z. C. Zhou, F. Y. Yang, S. Wang, L. Wang, X. F. Wang, C. Wang, Y. Xie, and Q. Liu, Emerging of two-dimensional materials in novel memristor, *Front. Phys.* 17(2), 23204 (2022)
4. C. J. Wan, G. Chen, Y. M. Fu, M. Wang, N. Matsuhisa, S. W. Pan, L. Pan, H. Yang, Q. Wan, L. Q. Zhu, and X. D. Chen, An artificial sensory neuron with tactile perceptual learning, *Adv. Mater.* 30(30), 1801291 (2018)
5. X. Liu, J. Zheng, D. Wang, P. Musavigharavi, E. A. Stach, R. III Olsson, and D. Jariwala, Aluminum scandium nitride-based metal-ferroelectric-metal diode memory devices with high on/off ratios, *Appl. Phys. Lett.* 118(20), 202901 (2021)
6. S. B. Ji, C. J. Wan, T. Wang, Q. S. Li, G. Chen, J. W. Wang, Z. Y. Liu, H. Yang, X. J. Liu, and X. D. Chen, Water-resistant conformal hybrid electrodes for aquatic endurable electrocardiographic monitoring, *Adv. Mater.* 32, 2001496 (26) (2020)
7. N. A. He, Y. M. Sun, and D. Z. Wen, Synaptic behavior

of Ni-Co layered double hydroxide-based memristor, *Appl. Phys. Lett.* 118(17), 173503 (2021)
8. S. W. Ke, L. Jiang, Y. F. Zhao, Y. Y. Xiao, B. Jiang, G. Cheng, F. C. Wu, G. S. Cao, Z. H. Peng, M. Zhu, and C. Ye, Brain-like synaptic memristor based on lithium-doped silicate for neuromorphic computing, *Front. Phys.* 17(5), 53508 (2022)
9. G. D. Zhou, X. D. Yang, L. H. Xiao, B. Sun, and A. K. Zhou, Investigation of a submerging redox behavior in Fe_2O_3 solid electrolyte for resistive switching memory, *Appl. Phys. Lett.* 96(11), 110404 (2006)
10. S. Lee, Y. T. Lee, S. G. Park, K. H. Lee, S. W. Kim, D. K. Hwang, and K. Lee, Dimensional crossover transport induced by substitutional atomic doping in $SnSe_2$, *Adv. Electron. Mater.* 4(4), 1700563 (2018)
11. B. Gao, J. F. Kang, L. F. Liu, X. Y. Liu, and B. Yu, A physical model for bipolar oxide-based resistive switching memory based on ion-transport-recombination effect, *Appl. Phys. Lett.* 98(23), 232108 (2011)
12. G. D. Zhou, Z. Wang, B. Sun, F. Zhou, L. Sun, H. Zhao, X. Hu, X. Peng, J. Yan, H. Wang, W. Wang, J. Li, B. Yan, D. Kuang, Y. Wang, L. Wang, and S. Duan, Volatile and nonvolatile memristive devices for neuromorphic computing, *Adv. Electron. Mater.* 8(7), 2101127 (2022)
13. I. Valov and M. N. Kozicki, Cation-based resistance change memory, *J. Phys. D* 46(7), 074005 (2013)
14. L. Goux and I. Valov, Electrochemical processes and device improvement in conductive bridge RAM cells, *Phys. Status Solidi. A* 213(2), 274 (2016)
15. F. Messerschmitt, M. Jansen, and J. Rupp, When memristance crosses the path with Humidity sensing — About the importance of protons and its opportunities in valence change memristors, *Adv. Electron. Mater.* 4, 1800282 (2018)
16. L. N. Du, Z. C. Wang, and G. Z. Zhao, Novel intelligent devices: Two-dimensional materials based memristors, *Front. Phys.* 17(2), 23602 (2022)
17. N. Matsuhisa, Y. Jiang, Z. Y. Liu, G. Chen, C. J. Wan, Y. Kim, J. Kang, H. Tran, H. C. Wu, I. You, Z. A. Bao, and X. D. Chen, High-transconductance stretchable transistors achieved by controlled gold microcrack morphology, *Adv. Electron. Mater.* 5(8), 1900347 (2019)
18. Y. M. Sun and D. Z. Wen, Logic function and random number generator build based on perovskite resistive switching memory and performance conversion via flexible bending, *ACS Appl. Electron. Mater.* 112, 102905 (2018)
19. Z. D. Luo, G. Apachitei, M. M. Yang, J. J. P. Peters, A. M. Sanchez, and M. Alexe, Bi-ferroic memristive properties of multiferroic tunnel junctions, *Appl. Phys. Lett.* 2, 618 (2020)
20. S. Zhu, B. Sun, G. D. Zhou, T. Guo, C. Ke, Y. Chen, F. Yang, Y. Zhang, J. Shao, and Y. Zhao, In-depth physical mechanism analysis and wearable applications of HfO_x-based flexible memristors, *ACS Appl. Mater. Interfaces* 15(4), 5420 (2023)
21. Z. R. Wang, M. Rao, J. W. Han, J. M. Zhang, P. Lin, Y. Li, C. Li, W. Song, S. Asapu, R. Midya, Y. Zhuo, H. Jiang, J. H. Yoon, N. K. Upadhyay, S. Joshi, M. Hu, J. P. Strachan, M. Barnell, Q. Wu, H. Wu, Q. Qiu, R. S. Williams, Q. Xia, and J. J. Yang, Capacitive neural network with neurotransistors, *Nat. Commun.* 9(1), 3208 (2018)
22. G. D. Zhou, J. G. Wu, L. D. Wang, B. Sun, Z. J. Ren, C. Y. Xu, Y. Q. Yao, L. P. Liao, G. Wang, S. H. Zheng, P. Mazumder, S. K. Duan, and Q. L. Song, Evolution map of the memristor: From pure capacitive state to resistive switching state, *Nanoscale* 11(37), 17222 (2019)
23. Z. C. Zhou, F. Y. Yang, S. Wang, L. Wang, X. F. Wang, C. Wang, Y. Xie, Q. Liu, Emerging of two-dimensional materials in novel memristor, *Front. Phys.* 17(2), 14, 23204 (2022)
24. X. B. Yan, H. D. He, G. J. Liu, Z. Zhao, Y. F. Pei, P. Liu, J. H. Zhao, Z. Y. Zhou, K. Y. Wang, and H. W. Yan, A robust memristor based on epitaxial vertically aligned nanostructured $BaTiO_3$–CeO_2 films on silicon, *Adv. Mater.* 34(23), 2110343 (2022)
25. G. D. Zhou, B. Sun, X. Hu, L. Sun, Z. Zou, B. Xiao, W. Qiu, B. Wu, J. Li, J. Han, L. Liao, C. Xu, G. Xiao, L. Xiao, J. Cheng, S. Zheng, L. Wang, Q. Song, and S. Duan, Negative photoconductance effect: An extension function of the TiO_x-based memristor, *Adv. Sci. (Weinh.)* 8(13), 2003765 (2021)
26. Z. R. Wang, S. Joshi, S. Savel'ev, W. H. Song, R. Midya, Y. N. Li, M. Y. Rao, P. Yan, S. Asapu, Y. Zhuo, H. Jiang, P. Lin, C. Li, J. H. Yoon, N. K. Upadhyay, J. Zhang, M. Hu, J. P. Strachan, M. Barnell, Q. Wu, H. Wu, R. S. Williams, Q. Xia, and J. J. Yang, Fully memristive neural networks for pattern classification with unsupervised learning, *Nat. Electron.* 1(2), 137 (2018)
27. X. Hu, W. Wang, B. Sun, Y. Wang, J. Li, and G. Zhou, Refining the negative differential resistance effect in a TiO_x-based memristor, *J. Phys. Chem. Lett.* 12(22), 5377 (2021)
28. W. Wang, G. D. Zhou, Y. Wang, B. Sun, M. Zhou, C. Fang, C. Xu, J. Don, F. Wang, S. Duan, and Q. L. Song, An analogue memristor made of silk fibroin polymer, *J. Mater. Chem. C* 9(41), 14583 (2021)
29. I. Valov and T. Tsuruoka, Effects of moisture and redox reactions in VCM and ECM resistive switching memories, *J. Phys. D* 51(41), 413001 (2018)
30. A. V. Valov, S. V. Golovin, V. V. Shcherbakov, and D. S. Kuznetsov, Thermoporoelastic model for the cement sheath failure in a cased and cemented wellbore, *J. Petrol. Sci. Eng.* 210, 109916 (2022)
31. T. Guo, J. Ge, Y. Jiao, Y. Teng, B. Sun, W. Huang, H. Asgarimoghaddam, K. P. Musselman, Y. Fang, Y. N. Zhou, and Y. A. Wu, Intelligent matter endows reconfigurable temperature and humidity sensations for in-sensor computing, Mater. Horiz., doi: 10.1039/D2MH01491B (2023)
32. B. Sun, Y. Chen, M. Xiao, G. Zhou, S. Ranjan, W. Hou, X. Zhu, Y. Zhao, S. A. T. Redfern, and Y. N. Zhou, A unified capacitive-coupled memristive model for the nonpinched current-voltage hysteresis loop, *Nano Lett.* 19(9), 6461 (2019)
33. G. D. Zhou, Z. Ren, B. Sun, J. Wu, Z. Zou, S. Zheng, L. Wang, S. Duan, and Q. Song, Capacitive effect: An original of the resistive switching memory, *Nano Energy* 68, 104386 (2020)
34. F. Messerschmitt, M. Kubicek, and J. L. M. Rupp, How does moisture affect the physical property of memristance for anionic-electronic resistive switching memories, *Adv. Funct. Mater.* 25(32), 5117 (2015)

35. G. Zhou, S. Duan, P. Li, B. Sun, B. Wu, Y. Yao, X. Yang, J. Han, J. Wu, G. Wang, L. Liao, C. Lin, W. Hu, C. Xu, D. Liu, T. Chen, L. Chen, A. Zhou, and Q. Song, Coexistence of negative differential resistance and resistive switching memory at room temperature in TiO_x modulated by moisture, *Adv. Electron. Mater.* 4(4), 1700567 (2018)
36. T. Tsuruoka, I. Valov, S. Tappertzhofen, J. van den Hurk, T. Hasegawa, R. Waser, and M. Aono, Redox reactions at Cu, Ag/Ta_2O_5 interfaces and the effects of Ta_2O_5 film density on the forming process in atomic switch structures, *Adv. Funct. Mater.* 25(40), 6374 (2015)
37. G. Milano, M. Luebben, M. Laurenti, L. Boarino, C. Ricciardi, and I. Valov, Structure-dependent influence of moisture on resistive switching behavior of ZnO thin Films, *Adv. Mater. Interfaces* 8(16), 2100915 (2021)
38. M. Lübben, S. Wiefels, R. Waser, and I. Valov, Processes and effects of oxygen and moisture in resistively switching TaO_x and HfO_x, *Adv. Electron. Mater.* 4(1), 1700458 (2018)
39. Y. Li and Y. Gao, Interplay between water and TiO_2 anatase (101) surface with subsurface oxygen vacancy, *Phys. Rev. Lett.* 112(20), 206101 (2014)
40. M. Lübben, S. Menzel, S. G. Park, M. Yang, R. Waser, and I. Valov, Set kinetics of electrochemical metallization cells: Influence of counter-electrodes in SiO_2/Ag based systems, *Nanotechnology* 28(13), 135205 (2017)
41. F. Zhou, Z. Zhou, J. Chen, T. H. Choy, J. Wang, N. Zhang, Z. Lin, S. Yu, J. Kang, H. P. Wong, and Y. Chai, Optoelectronic resistive random-access memory for neuromorphic vision sensors, *Nat. Nanotechnol.* 14(8), 776 (2019)
42. Y. F. Liu and L. Yobas, Microfluidic emulsification through a monolithic integrated glass micronozzle suspended inside a flow-focusing geometry, *Appl. Phys. Lett.* 106(17), 174101 (2015)
43. S. Tappertzhofen, I. Valov, T. Tsuruoka, T. Hasegawa, R. Waser, and M. Aono, Generic relevance of counter charges for cation-based nanoscale resistive switching memories, *ACS Nano* 7(7), 6396 (2013)
44. T. Tsuruoka, K. Terabe, T. Hasegawa, I. Valov, R. Waser, and M. Aono, Effects of moisture on the switching characteristics of oxide-based, gapless-type atomic switches, *Adv. Funct. Mater.* 22(1), 70 (2012)
45. M. D. Pickett, G. Medeiros-Ribeiro, and R. S. Williams, A scalable neuristor built with Mott memristors, *Nat. Mater.* 12(2), 114 (2013)
46. I. Valov, E. Linn, S. Tappertzhofen, S. Schmelzer, J. van den Hurk, F. Lentz, and R. Waser, Nanobatteries in redox-based resistive switches require extension of memristor theory, *Nat. Commun.* 4(1), 1771 (2013)
47. I. Valov, R. Waser, J. R. Jameson, and M. N. Kozicki, Electrochemical metallization memories-fundamentals, applications, prospects, *Nanotechnology* 22(25), 254003 (2011)
48. G. D. Zhou, X. Ji, J. Li, F. Zhou, Z. Dong, B. Yan, B. Sun, W. Wang, X. Hu, Q. Song, L. Wang, and S. Duan, Second-order associative memory circuit hardware implemented by the evolution from battery-like capacitance to resistive switching memory, *iScience* 25(10), 105240 (2022)
49. X. Hong, J. Hoffman, A. Posadas, K. Zou, C. H. Ahn, and J. Zhu, Unusual resistance hysteresis in n-layer graphene field effect transistors fabricated on ferroelectric $Pb(Zr_{0.2}Ti_{0.8})O_3$, *Appl. Phys. Lett.* 97(3), 033114 (2010)
50. Z. Guo, Y. D. Guan, Q. Luo, J. M. Hong, and L. You, Ferroelectric-nanocrack switches for memory and complementary logic with zero off-current and low operating voltage, *Adv. Electron. Mater.* 7(6), 2100023 (2021)
51. Q. Kang, C. Wang, S. Zhou, G. Li, T. Lu, Y. Tian, and P. He, Low-temperature co-hydroxylated Cu/SiO_2 hybrid bonding strategy for a memory-centric chip architecture, *ACS Appl. Mater. Interfaces* 13(32), 38866 (2021)
52. N. Pedisius, M. Praspaliauskas, J. Pedisius, and E. Dzenajaviciene, Analysis of wood chip characteristics for energy production in lithuania, *Energies* 14(13), 3931 (2021)
53. M. Hu, C. E. Graves, C. Li, Y. Li, N. Ge, E. Montgomery, N. Davila, H. Jiang, R. S. Williams, J. J. Yang, Q. Xia, and J. P. Strachan, Memristor-based analog computation and neural network classification with a dot product engine, *Adv. Mater.* 30(9), 1705914 (2018)
54. M. J. Jr Ellsworth, G. F. Goth, R. J. Zoodsma, A. Arvelo, L. A. Campbell, and W. J. Anderl, An overview of the IBM power 775 supercomputer water cooling system, *J. Electron. Packag.* 134(2), 020906 (2012)
55. G. Milano, E. Miranda, M. Fretto, I. Valov, and C. Ricciardi, Experimental and modeling study of metal-insulator interfaces to control the electronic transport in single nanowire memristive devices, *ACS Appl. Mater. Interfaces* 14(47), 53027 (2022)
56. O. C. Akgun, K. Nanbakhsh, V. Giagka, and W. A. Serdijn, A chip integrity monitor for evaluating moisture/ion ingress in mm-sized single-chip implants, *IEEE Trans. Biomed. Circuits Syst.* 14(4), 658 (2020)
57. C. Mannequin, T. Tsuruoka, T. Hasegawa, and M. Aono, Composition of thin Ta_2O_5 films deposited by different methods and the effect of humidity on their resistive switching behavior, *Jpn. J. Appl. Phys.* 55(6S1), 06GG08 (2016)
58. G. D. Zhou, B. Sun, Z. J. Ren, L. D. Wang, C. Y. Xu, B. Wu, P. Li, Y. Q. Yao, and S. Duan, Resistive switching behaviors and memory logic functions in single MnO_x nanorod modulated by moisture, *Chem. Commun. (Camb.)* 55(67), 9915 (2019)
59. G. D. Zhou, Z. Ren, L. Wang, J. Wu, B. Sun, A. Zhou, G. Zhang, S. Zheng, S. Duan, and Q. Song, Resistive switching memory integrated with amorphous carbon-based nanogenerators for self-powered device, *Nano Energy* 63, 103793 (2019)
60. J. Li, Y. Qian, W. Li, Y. Lin, H. Qian, T. Zhang, K. Sun, J. Wang, J. Zhou, Y. Chen, J. Zhu, G. Zhang, M. Yi, and W. Huang, Humidity-enabled organic artificial synaptic devices with ultrahigh moisture resistivity, *Adv. Electron. Mater.* 8(10), 2200320 (2022)
61. X. Ji, Z. Dong, C. Lai, G. Zhou, and D. Qi, A physics-oriented memristor model with the coexistence of NDR effect and RS memory behavior for bio-inspired computing, *Mater. Today Adv.* 16, 100293 (2022)